Insect Biochemistry and Molecular Biology 162 (2023) 104026

Contents lists available at ScienceDirect

Insect Biochemistry and Molecular Biology

journal homepage: www.elsevier.com/locate/ibmb

Pea aphid odorant-binding protein ApisOBP6 discriminates between aphid sex pheromone components, aphid alarm pheromone and a host plant volatile

Cassie Sims [a,b], Michael A. Birkett [a], Neil J. Oldham [b], Robert A. Stockman [b], David M. Withall [a,*]

[a] Protecting Crops and the Environment, Rothamsted Research, Harpenden, Hertfordshire, AL5 2JQ, UK
[b] School of Chemistry, University of Nottingham, University Park, Nottingham, NG7 2RD, UK

ARTICLE INFO

Keywords:
Insect olfaction
Pheromones
Odorant-binding protein
Aphids
Protein NMR
Molecular docking

ABSTRACT

Olfactory perception of pheromones in insects involves odorant-binding proteins (OBPs), relatively small proteins (ca.110-240 amino acid residues) that can bind reversibly to behaviourally active olfactory ligands. In this study, we investigated the binding *in silico* and *in vitro* of the aphid sex pheromone components (1*R*,4a*S*,7*S*,7a*R*)-nepetalactol and (4a*S*,7*S*,7a*R*)-nepetalactone and the aphid alarm pheromone (*E*)-β-farnesene by OBPs from the pea aphid, *Acyrthosiphon pisum*. Screening of protein models of ApisOBPs1-11 with the aphid sex pheromone components suggested that ApisOPB6 was a candidate. Fluorescence assays using ApisOBP6 suggested that ApisOBP6 was able to bind both sex pheromone components and discriminate from the aphid alarm pheromone and the generic plant compound (*R/S*)-linalool. Saturation transfer difference NMR experiments with ApisOBP6 yielded results consistent to those from the fluorescence experiments, with a clear interaction between ApisOBP6 and (4a*S*,7*S*,7a*R*)-nepetalactone. These results describe a novel interaction and potential function for ApisOBP6, point to pre-receptor odorant discrimination by OBPs, and provide a platform for investigating the function of other aphid olfactory proteins involved in aphid chemical ecology.

1. Introduction

Aphids (Homoptera: Aphididae) are economically important pests of horticultural and agricultural crops worldwide, causing damage both directly and indirectly through their feeding behaviour and transmission of detrimental plant viruses, such as barley yellow dwarf virus (BYDV) (Harris and Maramorosch, 1977; Pickett et al., 2013). Pheromones and other semiochemicals are naturally-occurring behaviour-modifying chemical signals that play a critical role in the life cycle of aphids (Pickett et al., 2013). Sex pheromones for aphid pest species principally comprise (1*R*,4a*S*,7*S*,7a*R*)-nepetalactol **1** and (4a*S*,7*S*,7a*R*)-nepetalactone **2**, whilst the main component of the aphid alarm pheromone for many pest aphids is (*E*)-β-farnesene **5**, and (*R/S*)-linalool **6** is utilised as host plant volatile cue (Fig. 1) (Dawson et al., 1987; Marsh, 1972; Pickett and Griffiths, 1980).

A number of studies have shown that olfactory perception of semiochemicals in insects involves at least two distinct groups of protein, i.e. olfactory receptors (ORs), seven transmembrane receptors with an inverse topology to the G-coupled protein receptors (GPCRs) found in mammals (Benton, 2006; Buck and Axel, 1991; Butterwick et al., 2018; del Mármol et al., 2021), and odorant-binding proteins (OBPs), relatively small proteins (ca. 110–240 amino acid residues) found in high concentrations (ca. 10 mM) in the sensillum lymph of antennae (Pelosi and Maida, 1995; Vogt and Riffiford, 1981; Zhou et al., 2010). Insect OBPs can be categorised into three distinct categories including classic OBPs (possessing 6 highly conserved cysteine residues), Plus-C OBPs (possessing 8 conserved cysteine residues and one conserved proline) and Atypical OBPs (possessing 9 or 10 conserved cysteine residues) (Zhou et al., 2010). Evidence of a role for OBPs in insect olfaction has been provided by deletion of OBPs in the striped rice stem borer, *Chilo suppressalis*, the tobacco cutworm, *Spodoptera litura*, and the common fruit fly, *Drosophila melanogaster*, resulting in significant reduction in antennal electrophysiological responses, measured by observing olfactory receptor neuron (ORN) responses to their respective binding ligands

Abbreviations: OBP, odorant-binding protein; ApisOBP, *Acyrthosiphon pisum* odorant-binding protein; OR, odorant receptor; STD-NMR, saturation transfer difference nuclear magnetic resonance.

* Corresponding author.
E-mail address: David.withall@rothamsted.ac.uk (D.M. Withall).

https://doi.org/10.1016/j.ibmb.2023.104026
Received 14 June 2023; Received in revised form 6 October 2023; Accepted 8 October 2023
Available online 11 October 2023

(Chang et al., 2015, p. 201; Dong et al., 2017; Larter et al., 2016; Zhu et al., 2016). For the pea aphid, *Acyrthosiphon pisum*, olfactory proteins ApisOBP3, ApisOBP7 and ApisOR5 have previously been shown to be critical for perception of the aphid alarm pheromone **5** (Northey et al., 2016; Qiao et al., 2009; Zhang et al., 2017). Concurrent to these studies, in this work we tested the hypothesis that *A. pisum* OBPs play a critical role in discrimination between sex pheromone components **1** and **2**, alarm pheromone **5** and host plant volatile cue **6**, using *in silico* modelling methods, fluorescence binding assays, STD-NMR experiments and biphasic gas chromatography assays. We also investigated the potential of aphid OBPs to discriminate between **1** and **2** and their non naturally-occurring stereoisomers **3** and **4**.

2. Materials and methods

2.1. Homology models

For ApisOBP1-11, protein structures were initially predicted using the iTASSER database, which takes a hierarchical approach by identifying structural templates from the Protein Data Bank. All predicted protein structures were minimised using the Yasara minimisation server. All homology models were visualised in PyMol 2.3.4.

2.2. Molecular docking

Ligands were prepared in Chem3D 16.0 and AutoDock 4.2. Docking studies were performed using AutoDock4.2 with the Racoon Virtual screening tool using a Lamarckian genetic algorithm. Binding energies and predicted K_i values were calculated through the virtual screening tool.

2.3. Production of OBPs

ApisOBP6 and ApisOBP9 were expressed in *E. coli*. A hexa-histidine tag and ampicillin resistance gene were included. Bl21 (DE3) competent *E. coli* were transformed with the plasmids of interest. Transformation was confirmed with colony selection, PCR and induction tests. Recombinant BL21 (DE3) *E. coli* was grown in LB media and expression induced with ITPG (Flurochem). Cell pellets were lysed by sonication in TBS and 0.2% Triton X-100 in TBS. After centrifugation, protein was initially denatured with 8 M urea and 100 mM DTT, then refolded *via* rapid dilution overnight with 0.5:5 mM GSSG:GSG. The final mixture was purified using a HiTrap nickel-affinity column (GE Healthcare) and elution with 500 mM imidazole. The His-Tag was removed *via* overnight cleavage with enterokinase (New England Biolabs) in 2 mM $CaCl_2$ in TBS and ApisOBP6/OBP9 further purified using a nickel-affinity column and fast-protein liquid chromatography (Akta) with a Superdex S200 column in TBS. The final protein was concentrated and buffer-exchange into 25 mM Tris using VivaSpin 20.

2.4. Synthetic chemistry

Synthetic chemistry methods and analysis can be found in Appendix B.

2.5. Fluorescence measurements

All fluorescent measurements were undertaken using a PerkinElmer LS50B fluorescence spectrophotometer, using a 2 mL quartz cuvette, unless otherwise stated. Spectra were recorded using FL WinLab software. Saturation of OBPs with fluorescent probe, 1-NPN (Sigma-Aldrich) was initially measured by titrating a 2 μM protein sample (2 mL in 25 mM Tris-HCl) with aliquots of 1 mM ligand in methanol to final concentrations of 1–16 μM. The fluorescence intensity was recorded. Titrations were performed with aliquots of 1 mM ligand in methanol to final concentrations of 1–20 μM, either after the addition of fluorescent probe to a final concentration of 1 μM or in the absence of fluorescent probe. To generate K_D values, relative fluorescence intensity was plotted against the concentration of ligand as a binding curve. K_D values were generated in GraphPad Prism 7 using a non-linear regression.

2.6. STD-NMR

Samples were run using an AVANCE Bruker DRX-500 MHz Nuclear Magnetic Resonance spectrometer equipped with a 5 mm BBO BB-1H probe and set at 500 MHz for ^{1}H spectra. Analysis of Bruker data was performed using Topspin 4.0.7.

STD-NMR samples comprised of ApisOBP6 (30 μM in D_2O) and ligand (3 mM in d_6-DMSO). The ApisOBP6 on-resonance frequency of 160 Hz was selected to ensure no accidental excitation of ligand signals. A 3 s saturation time and 5.12 s relaxation delay were used. For each run, 192 scans were performed. Off-resonance spectra were recorded with an excitation frequency of −12,000 Hz. STD absolute values were calculated by observing the change in proportions between the off-resonance spectrum and the final STD spectrum using the equation $(I_0\text{-}I_{STD})/I_0$ in which the term $(I_0 - I_{STD})$ represents the ratio of peak intensity in the STD spectrum and I_0 the ratio of intensity in the off resonance spectrum. A second value representing the proportionate change was calculated using the equation $I_0 - (I_0 - I_{STD})$.

2.7. Biphasic binding assay

High resolution gas chromatography-flame ionization detector (GC-FID) analysis was performed using an Agilent 6890A GC instrument

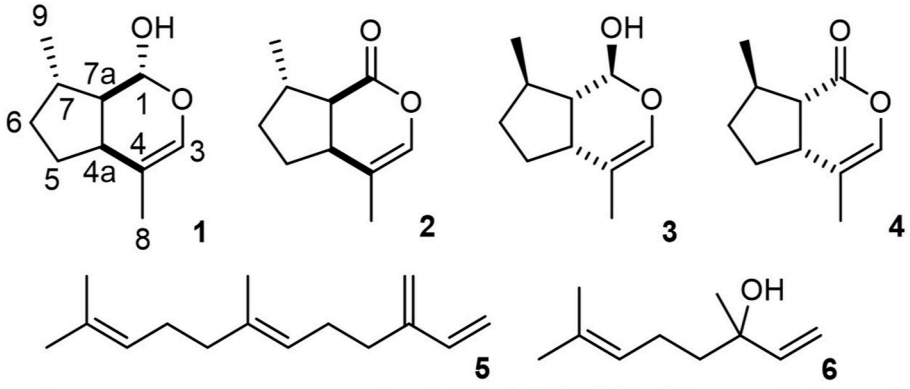

Fig. 1. Aphid sex pheromone components, (*1R,4aS,7S,7aR*)-nepetalactol **1** and (*4aS,7S,7aR*)-nepetalactone **2,** non-natural enantiomers of the sex pheromone components (*1S,4aR,7R,7aS*)-nepetalactol **3** and (*4aR,7R,7aS*)-nepetalactone **4,** the aphid alarm pheromone (*E*)-β-farnesene **5** and the generic host plant volatile (*R/S*)-linalool **6**.

equipped with a split/splitless injector and HP-1 column (320.00 μm diameter x 50 m length). The carrier gas was hydrogen (flow rate of 3.1 mL min^{-1}) and the GC oven temperature programmed to start at 30 °C, rise to 100 °C at a rate of 5 °C min^{-1}, maintained at 100 °C for 10 min, then rise again to 250 °C at a rate of 10 °C $min^{-1,}$ after which it was maintained at 250 °C for 45 min. The final run time was 84.10 min.

For the biphasic assay, a solution of test ApisOBP (100 μL of 5 μM in 25 mM Tris) was added to a glass vial (2 mL size). A ligand solution (80 μL of 12 μM solution in hexane) was carefully added on top, to create a biphasic system. The vial was gently mixed before being centrifuged (5,000 rpm, 15 min). Finally, samples were incubated (ambient temperature, 2h) and a sample (2 μL) of the hexane layer was removed and analysed by GC-FID. Quantification of the amount of ligand per sample was undertaken by generating a calibration curve for each ligand across a range of concentrations (Supplemental Data Fig. S2). The amount of ligand present was reported in milligram and micromolar quantities.

2.8. Statistical analysis

Statistical analysis was performed in R 3.4.4. For fluorescence data, a one-way weighted analysis of variance (ANOVA) was performed between ligands for each protein, and a two-way weighted ANOVA was performed to investigate the interactions between proteins and ligands. For gas chromatography, a two-way ANOVA was performed. In both analyses, a Tukey Test was used for post-hoc analysis.

3. Results and discussion

3.1. In silico predictions

Initially, *in silico* modelling was adopted to identify potential discriminatory binding interactions between *A. pisum* OBPs and compounds **1**–**6**. Three-dimensional protein models of ApisOBPs 1–11 were generated using iTASSER, minimised using the Yasara minimisation server and visualised in PyMol (Fig. 2) (Krieger et al., 2009; Pandit et al., 2006; Schrödinger, 2015). The generated homology models were screened using AutoDock 4.2 for their predicted interaction with **1**–**6** (Fig. 3) (Forli et al., 2016; Morris et al., 1998).

Significantly stronger binding of ApisOBP6 with sex pheromone components **1** and **2** was predicted compared to the alarm pheromone **5** and the plant volatile cue **6**. Other ApisOBPs were predicted to have relatively weaker binding affinities for **1, 2, 5** and **6**, with ApisOBP9 displaying the lowest predicted energy interactions. This was also reflected in the calculated K_I values, with the lowest K_I for the sex pheromone component **1** being 2.3 μM and the K_I for **5** being predicted at a higher 11.5 μM. Non-naturally occurring stereosiomers **3** and **4** were predicted to bind with similar energy as sex pheromone components **1** and **2**. From these predictions, ApisOBP6 was selected as a candidate for *in vitro* experiments to confirm predicted discrimation ability, and ApisOBP9 was selected as a control protein, due to predicted low-affinity binding activity.

3.2. Fluorescence assays

Recombinant ApisOBP6 and ApisOBP9 were prepared *via* cloning of the required genes, transformation of pET45b *E. coli* expression system and affinity purification followed by subsequent cleavage of His_6 tag. Authentic samples of **1**–**6** were obtained with the aim of studying the *in vitro* binding activity of ApisOBP6 and ApisOBP9 compared to predicted binding in the *in silico* modelling. Sex pheromone component **2** was purified from *Nepeta cataria* essential oil by flash column chromatography, whilst **1** was synthesised from **2** by stereoselective sodium borohydride reduction (Appendix B) (Birkett and Pickett, 2003). Non-naturally occurring steroisomer **3** was synthesised *via* a multi-step synthesis starting from commercially avaliable (*R*)-citronellol **7** (Dawson et al., 1996; Schreiber et al., 1986). Allylic oxidation with catalytic

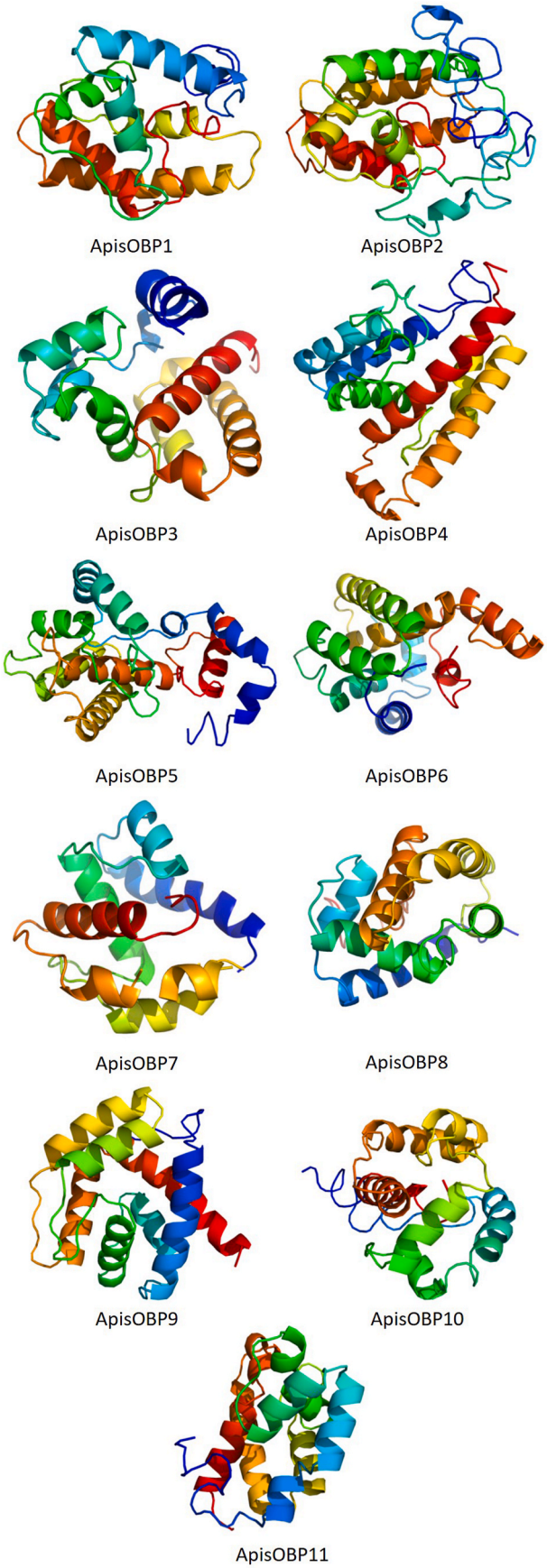

Fig. 2. Homology model of *Acyrthosiphon pisum* odorant-binding protein 1-11 (ApisOBP1-11) generated with iTASSER and PyMol.

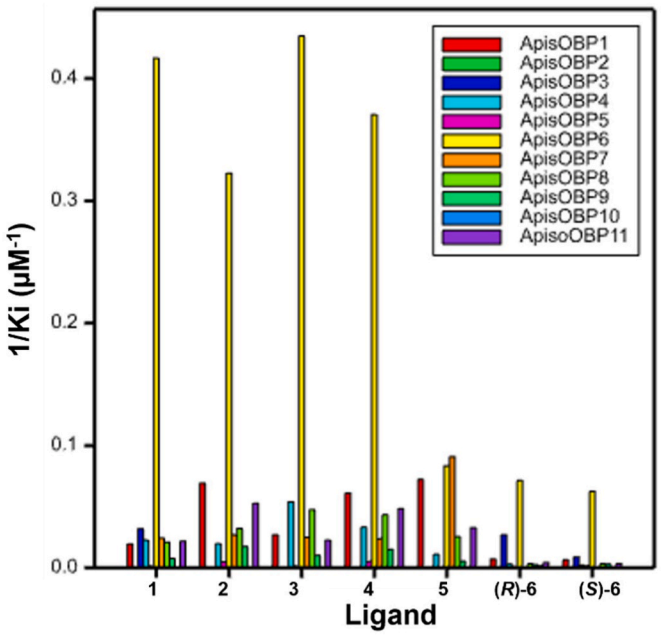

Fig. 3. Predicted *in silico* binding interactions (shown as $1/K_i$) of key aphid semiochemicals **1**–**6** with ApisOBP1-11.

selenium dioxide followed by Swern oxidation yielded dialdehyde **8**. Cyclisation of dialdehyde **8** proceeded via an intramolecular enamine-mediated [4 + 2] cycloadition to yield cyclised product **9**. Hydrolysis of **9** yielded non-naturally ocurring steroisomer **3** that was converted to **4** via Fétizon oxidation (Appendix B). Alarm pheromone **5** was prepared by the regioselective 1,4-elimination of the allylic ether THP-(*E, E*)-farnesol as previously reported (Kang et al., 1987), while (*R/S*)-linalool **6** was commercially available (Sigma Aldrich).

In vitro fluorescence binding studies with ApisOBP6 were conducted through monitoring displacement of a fluorescent probe *N*-phenyl-1-naphthylamine (1-NPN) by **1**–**6** (Qiao et al., 2009). The sex pheromone components **1** and **2** and stereoisomers **3** and **4** yielded binding data to ApisOBP6 consistent with the predicted values from the *in silico* modelling, indicating that the protein models have a high degree of accuracy. A significant difference in binding was observed when comparing **1**–**4** with the alarm pheromone **5** and the plant volatile cue **6** (Fig. 4a). The interaction between ApisOBP6 and sex pheromone component **2** provided the lowest K_D value with 1.3 ± 0.6 μM. There was no statisitcal difference between binding constants of the naturally occurring sex pheromone components **1** and **2** and thier corresponding stereoisomers **3** and **4**. However, there was a potential difference between **2** and **4** ($p = 0.11$), althought this was not statistically significant. There was no statistical difference in measured binding constants between aphid semiochemicals **1**–**5** and ApisOBP9 (Fig. 4b). This apparent stereoselectivity trend of ApisOBP6 is consistent with previously reported literature of other insect OBPs. In the gypsy moth, *Lymantria dispar*, LdisOBP1 was shown to preferentially bind (−)-disparlure while LdisOBP2 preferentially bound (+)-disparlure (Plettner et al., 2000). Futhermore, Plettner et al. demonstrated that ApolOBP3, from *Antheraea polyohemus,* exhibited a lower binding affinity towards (+)-disparlure compared to (−)-disparlure. Contrastingly however, OBPs from the Japanese beetle, *Popillia japnica*, and the Osaka beetle, *Anomala osakana*, are incapable of discriminating between the stereoisomers of japonilure, even though both beetles behaviourally discriminate the respective japonilure enantiomers (Wojtasek et al., 1998). Given these previously reported observations, in combination with our results detailed here, they suggest that the molecular mechanism of insect semiochemical enantiodiscrimination is still not fully understood and potentially involves other olfactory proteins, such as odorant receptors, to fully account for the discrimination observed.

3.3. STD-NMR

STD-NMR experiments were performed to further explore *in vitro* binding between ApisOBP6 and **2** and **5**, selected as the strongest binder and non-binder to ApisOBP6 respectively (Fig. 5) (Mayer and Meyer, 1999; Xia et al., 2010). For sex pheromone component **2**, strong positive STD-spectra were observed for resonances 1.21, 1.50–1.59, 1.64, 1.89–1.98, 2.02–2.11, 2.31–2.39 and 2.05 ppm while resonance 6.18–6.20 ppm had a negative difference. For **5**, only weak positive difference spectra were observed for resonances 1.48, 1.52 and 4.95 ppm. STD-NMR experiments clearly demonstrated an interaction between ApisOBP6 and **2** while only non-specific interactions were observed betweenApisOBP6 and **5**. Epitope mapping of the attenuation of individual resonances in **2** revealed the greatest attenuation for the two methyl substituents, with all the cyclopentyl protons also demonstrating different degrees of attenuation (Fig. 5). Epitope mapping of the attenuation of individual protons of **2** was consistent with a binding conformation predicted from the *in silico* modelling (Fig. 6) (Mayer and Meyer, 2001). Greatest attentuation of the two methyl substitents of **2** was consistent with predicted binding conformation given these substituents point directly at the protein surface, while the cyclopentyl protons also experience attenuation being located deep within the binding pocket. Proton 6.18–6.20 ppm of **2** showed minimal attenuation in the STD-NMR, consistent with the predicted binding orientation positioning this proton directly towards the binding pocket opening and therefore having minimal interactions with the protein. This low

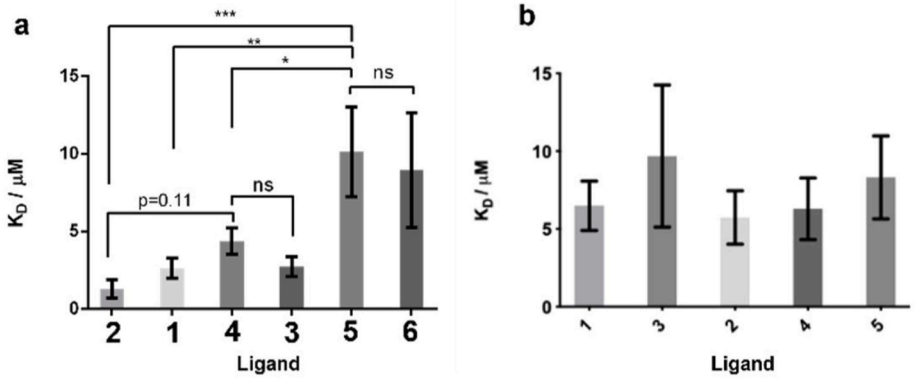

Fig. 4. Binding constants between (a) ApisOBP6 and (b) ApisOBP9 and aphid semiochemicals (4aS,7S,7aR)-nepetalactone **2**, (4aR,7R,7aS)-nepetalactone **4**, (1R,4aS,7S,7aR)-nepetalactol **1**, (1S,4aR,7R,7aS)-nepetalactol **3,** (*E*)-β-farnesene **5** and (R/S)-linalool **6** calculated from fluorescence data. * = $p < 0.05$; ** = $p < 0.01$; *** = $p < 0.001$; ns = no significance.

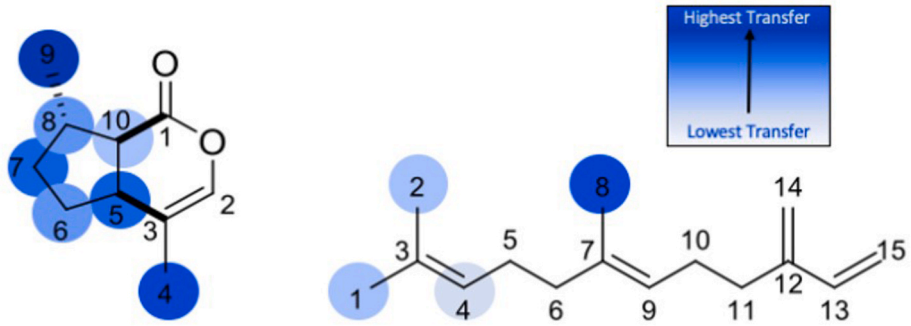

Fig. 5. **2** showing the predicted epitope mapping (blue) when bound to ApisOBP6 and **5** showing the predicted non-specific interactions (blue) when interacting with ApisOBP6. Raw values found in Supplementary Data (Table S2; Fig. S1).

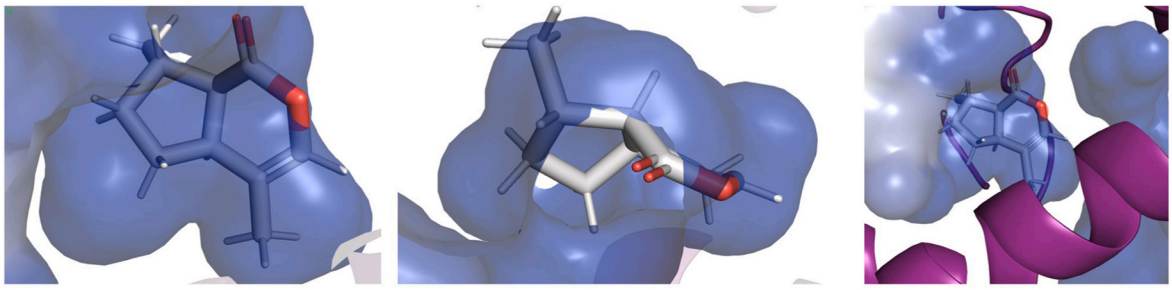

Fig. 6. (4a*S*,7*S*,7a*R*)-Nepetalactone **1** (white, with oxygens in red) in the predicted binding pocket of ApisOBP6 (blue/purple).

attenuation could also be explained by solvent molecules blocking the interactions with the protein as previously described and was again consistent with proton-2 being located at the binding pocket opening (Brecker et al., 2006; Mayer and Meyer, 2001; Puchner et al., 2015).

STD-NMR demonstrates which protons are involved in the binding interaction by measuring distance dependence saturation-transfer. STD-NMR spectra demonstrated a clear interaction between ApisOBP6 and **2**, and a lack of specific interaction between ApisOBP6 and the alarm pheromone **5**. The lack of a difference spectra for **5**, indicating a lack of binding suggesting that ApisOBP6 can discriminates the sex pheromone component from other important aphid semiochemicals. Proton resonances for almost all protons of **2** remained in the final STD-NMR spectrum, suggesting that a saturation transfer between the protein and ligand had occurred. Conversely, the STD-NMR spectrum for ApisOBP6 and **5** showed only a few remaining peaks, which can be explained by non-specific interactions of the protruding methyl groups. An unusual result was observed with the alkene proton at the C-2 position, in which a negative STD-NMR spectrum was recorded. This negative difference peak has been observed in other STD-NMR experiments and was previously explained as due to a solvent molecule interfering with the saturation of the ligand during spin and lock time (Mayer and Meyer, 2001; Puchner et al., 2015). From our *in silico* modelling data, proton 2-H of **2** is protruding out of the predicted pocket into the aqueoues external environment and is therefore accessible to solvent interferance (Fig. 6). In previous literature, this effect has been observed with lactose ring structure, similar to the lactone structure seen here (Brecker et al., 2006).

3.4. Biphasic binding assay

Biphasic gas chromatography assays were carried out with ApisOBP6, ApisOBP9 and compounds **1**, **2** and **5** presented in aqueous/

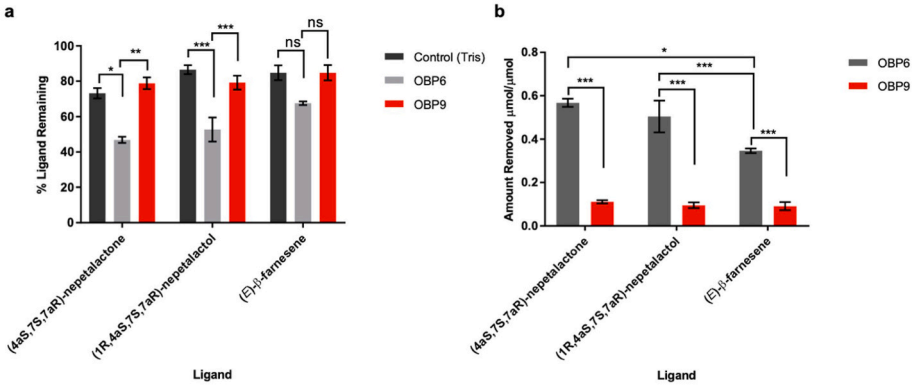

Fig. 7. **(a)** The percentage change in amount of ligand in the biphasic assay as monitored by gas chromatography of ApisOBP6 and ApisOBP9 compared to a control (Tris); **(b)** The amount of ligand (µmol) removed from the layer per protein (µmol). For statistical analysis, * = $p < 0.05$; ** = $p < 0.01$; *** = $p < 0.001$; ns = no significance.

hexane phases respectively as a mimic of the natural biphasic system found *in vivo* (Fig. 7) (Zhou et al., 2009). Significant differences in the amount of compound removed from the hexane layer, and the amount removed relative to the amount of protein present, were observed when hexane layers were combined with aqueous layers containing ApisOBP6, ApisOBP9 or no protein. The presence of ApisOBP6 in the aqueous layer resulted in a significantly greater removal of **1** and **2,** but not **5,** from the hexane layer compared to the presence of ApisOBP9 or no protein at all. Furthermore, the ratio of ligand (μmol per μmol protein) removed from the hexane layer was significantly higher when ApisOBP6 was present in the aqueous layer compared to when ApisOBP9 was present.

No clear differences between the control samples and the sample containing ApisOBP9 were observed. However, with ApisOBP6, the amount of **1** and **2** in the hexane layer reduced to a significantly lower level than in the control or ApisOBP9. Furthermore, the ratio of molar quantities of **1** and **2** taken up per mole of OBP was significantly higher in ApisOBP6 than with ApisOBP9.

4. Conclusion

Due to the high levels of background noise experienced by the insect olfactory system in the wild and the high level of specificity required, insect olfactory proteins must be sophisticated in their ability to recognise and discriminate between molecules in comparison to other recognition proteins (Touchet et al., 2015). Recently, OBPs and ORs from *A. pisum,* ie. ApisOBP3, ApisOBP7 and ApisOR5, were shown to be critical for perception of the aphid alarm pheromone, (*E*)-β-farnesene **5** (Northey et al., 2016; Wang et al., 2021; Zhang et al., 2017). Our results show that not only can ApisOBP6 bind the aphid sex pheromone components **1** and **2** and their respective non naturally-occurring stereoisomers **3** and **4**, but ApisOBP6 can also discriminate from the aphid alarm pheromone **5** and the generic host plant volatile (*R/S*)-linalool **6**. Furthermore, we observed a possible trend that ApisOBP6 has minor stereoselectivity towards the naturally occurring stereoisomers over the biologically inactive non-natural stereoisomer, although this was not statistically significant. To our knowledge this is the first report of an interaction between an aphid OBP and aphid sex pheromone component and discrimation between different aphid semiochemicals at the olfactory level. ApisOBP6 is one of only two Plus-C OBPs found in aphids and is responsible for the second most abundant OBP mRNA in aphid antennae (De Biasio et al., 2014). It is also a large OBP at 215 residues; it has been suggested that larger OBPs may have a longer C-terminal region, which can contribute to a conformational change by folding into the binding pocket when a ligand is bound (Gomez-Diaz et al., 2013; Pesenti et al., 2008; Zhang et al., 2017).

In addition to exploring the ability of aphid OBPs to discriminate between multiple different semiochemicals, we also explored their ability to discriminate between stereoisomers. The enantiomers of the sex pheromone components **3** and **4** were tested *in silico* and *in vitro* with fluorescence binding assays. There was no significant difference between the sex pheromone components **2** and its enantiomers **4** interaction with ApisOBP6. This apparent slight ability of ApisOBP6 to distinguish between enantiomers of the sex pheromone components suggests that another olfactory protein, most likely an OR, is responsible for enantiomeric discrimination. Although it is difficult to elucidate the role of ApisOBPs from these initial results, the slight differences observed should be investigated further. If true enantiomeric differences are seen, this would be one of the first observation of OBPs playing a discriminating role at this level (Sun et al., 2012). Future work should focus on the deorphanisation of ORs in *A. pisum* to find a potential corresponding sex pheromone OR that may interact with ApisOBP6.

After the success of the fluorescence binding studies between ApisOBP6 and the sex pheromone components **1** and **2**, STD-NMR experiments and biphasic binding assays were explored to delve deeper into the specifics of the ApisOBP6 and aphid pheromone interactions. The biphasic assay was uniquely designed to provide a more realistic method for investigating OBP binding activities, specifically investigating polyphasic systems present in the sensory organs. Solubilising ligands, typically hydrophobic in nature, from the air via the cuticular wax coated antennal pore into an aqueous solution (the sensillum lymph) is one of the main roles hypothesized for OBPs (Pelosi et al., 2006). Overall, these results indicate ApisOBP6 increases the amount of **1** and **2** that can be solubilised into the aqueous layer than with a control or ApisOBP9. This result is consistent with the other ligand binding assays with ApisOBP6, and further supports the role of ApisOBP6 in binding sex pheromone components **1** and **2**.

In summary, our data shows that ApisOBP6, an OBP from the pea aphid, *A. pisum*, can discriminate between aphid sex pheromone components **1** and **2**, the aphid alarm pheromone **5** and the generic host plant volatile cue **6.** We also observed a slight trend, although not statistically significant, in stereoselectivity between biologically active natural stereoisomers and the non-naturally occurring bioligcally inactive stereoisomer that suggests the role of another component of the olfactory system, potentially an OR. Our results suggest that ApisOBP6 may play a role in the perception of the aphid sex pheromone and a possible role in pre-receptor odorant filtering. The work also demonstrates successful prediction of pheromone-OBP interactions generated from *in silico* modelling and indicates a new NMR-based method for exploring olfactory protein-ligand interactions. Both these approaches may be deployed in the study of the function of other insect olfactory proteins. Further work including X-ray crystallography, RNAi-based silencing or CRISPR/Cas9 is required to confirm ApisOBP6 function *in vivo* and the potential role of an OR in enantiomeric discrimination of chiral aphid sex pheromone components.

Funding

CS was supported by a Biotechnology and Biological Sciences (BBSRC) Doctoral Training Programme (DTP) studentship (reference 1804053). Rothamsted Research receives strategic funding from the Biotechnology and Biological Sciences Research Council of the United Kingdom (BBSRC). We acknowledge support from the Smart Crop Protection strategic programme (BBS/OS/CP/000001) funded through BBSRC's Industrial Strategy Challenge Fund, and the Growing Health Institute Strategic Programme (BB/X010953/1).

Declaration of competing interest

The authors declare that they have no conflicts of interest with the contents of this article.

Acknowledgments

We are grateful to Professor Jing-Jiang Zhou for providing plasmids from earlier strategic-funded work at Rothamsted Research.

Appendix A. Supplementary data

Supplementary data to this article can be found online at https://doi.org/10.1016/j.ibmb.2023.104026.

References

Benton, R., 2006. On the ORigin of smell: odorant receptors in insects. Cell. Mol. Life Sci. 63, 1579–1585. https://doi.org/10.1007/s00018-006-6130-7.

Birkett, M.A., Pickett, J.A., 2003. Aphid sex pheromones: from discovery to commercial production. Phytochemistry 62, 651–656. https://doi.org/10.1016/S0031-9422(02)00568-X.

Brecker, L., Straganz, G.D., Tyl, C.E., Steiner, W., Nidetzky, B., 2006. Saturation-transfer-difference NMR to characterize substrate binding recognition and catalysis of two broadly specific glycoside hydrolases. J. Mol. Catal. B Enzym. 42, 85–89. https://doi.org/10.1016/j.molcatb.2006.07.004.

Buck, L., Axel, R., 1991. A novel multigene family may encode odorant receptors: a molecular basis for odor recognition. Cell 65, 175–187. https://doi.org/10.1016/0092-8674(91)90418-X.

Butterwick, J.A., del Mármol, J., Kim, K.H., Kahlson, M.A., Rogow, J.A., Walz, T., Ruta, V., 2018. Cryo-EM structure of the insect olfactory receptor Orco. Nature 560, 447–452. https://doi.org/10.1038/s41586-018-0420-8.

Chang, H., Liu, Y., Yang, T., Pelosi, P., Dong, S., Wang, G., 2015. Pheromone binding proteins enhance the sensitivity of olfactory receptors to sex pheromones in *Chilo suppressalis*. Sci. Rep. 5, 13093 https://doi.org/10.1038/srep13093.

Dawson, G., Griffiths, D., Janes, N., 1987. Identification of an aphid sex pheromone. Nature. https://doi.org/10.1038/325614a0.

Dawson, G.W., Pickett, J.a., Smiley, D.W.M., 1996. The aphid sex pheromone cyclopentanoids: synthesis in the elucidation of structure and biosynthetic pathways. Bioorg. Med. Chem. 4, 351–361. https://doi.org/10.1016/0968-0896(96)00012-0.

De Biasio, F., Riviello, L., Bruno, D., Grimaldi, A., Congiu, T., Sun, Y.F., Falabella, P., 2014. Expression pattern analysis of odorant-binding proteins in the pea aphid *Acyrthosiphon pisum*. Insect Sci. 1–15. https://doi.org/10.1111/1744-7917.12118, 00.

del Mármol, J., Yedlin, M.A., Ruta, V., 2021. The structural basis of odorant recognition in insect olfactory receptors. Nature. https://doi.org/10.1038/s41586-021-03794-8.

Dong, X.-T., Liao, H., Zhu, G.-H., Khuhro, S.A., Ye, Z.-F., Yan, Q., Dong, S.-L., 2017. CRISPR/Cas9 mediated PBP1 and PBP3 mutagenesis induced significant reduction in electrophysiological response to sex pheromones in male Chilo suppressalis. Insect Sci. 276, 1–10. https://doi.org/10.3389/fevo.2017.00142.

Forli, S., Huey, R., Pique, M.E., Sanner, M., Goodsell, D.S., Arthur, J., 2016. Computational protein-ligand docking and virtual drug screening with the AutoDock suite. Nat. Protoc. 11, 905–919. https://doi.org/10.1038/nprot.2016.051. Computational.

Gomez-Diaz, C., Reina, J.H., Cambillau, C., Benton, R., 2013. Ligands for pheromone-sensing neurons are not conformationally activated odorant binding proteins. PLoS Biol. 11 https://doi.org/10.1371/journal.pbio.1001546.

Harris, K.F., Maramorosch, K., 1977. Aphids as Virus Vectors. Academic, New York.

Kang, S.-K., Chung, G.-Y., Lee, D.-H., 1987. A convenient synthesis of (E)-β-Farnesene. Bull. Kor. Chem. Soc. 8, 351–353.

Krieger, E., Joo, K., Lee, Jinwoo, Lee, Jooyoung, Raman, S., Thompson, J., Tyka, M., Baker, D., Karplus, K., 2009. Improving physical realism, stereochemistry, and side-chain accuracy in homology modeling: four approaches that performed well in CASP8. Proteins: Struct., Funct., Bioinf. 77, 114–122. https://doi.org/10.1002/prot.22570.

Larter, N.K., Sun, J.S., Carlson, J.R., 2016. Organization and function of *Drosophila* odorant binding proteins. Elife 5, e20242. https://doi.org/10.7554/eLife.20242.

Marsh, D., 1972. Sex pheromone in the aphid *Megoura viciae*. Nature 238, 31–32. https://doi.org/10.1038/newbio238031a0.

Mayer, M., Meyer, B., 2001. Group epitope mapping by saturation transfer difference NMR to identify segments of a ligand in direct contact with a protein receptor. J. Am. Chem. Soc. 123, 6108–6117. https://doi.org/10.1021/ja0100120.

Mayer, M., Meyer, B., 1999. Characterization of ligand binding by saturation transfer difference NMR spectroscopy. Angew. Chem. Int. Ed. 38, 1784–1788. https://doi.org/10.1002/(SICI)1521-3773(19990614)38:12<1784::AID-ANIE1784>3.0.CO;2-Q.

Morris, G.M., Goodsell, D.S., Halliday, R.S., Huey, R., Hart, W.E., Belew, R.K., Olson, A. J., 1998. Automated docking using a Lamarckian genetic algorithm and an empirical binding free energy function. J. Comput. Chem. 19, 1639–1662.

Northey, T., Venthur, H., De Biasio, F., Chauviac, F.X., Cole, A., Ribeiro, K.A.L., Grossi, G., Falabella, P., Field, L.M., Keep, N.H., Zhou, J.J., 2016. Crystal structures and binding dynamics of odorant-binding protein 3 from two aphid species Megoura viciae and Nasonovia ribisnigri. Sci. Rep. 6, 1–13. https://doi.org/10.1038/srep24739.

Pandit, S.B., Zhang, Y., Skolnick, J., 2006. TASSER-lite: an automated tool for protein comparative modeling. Biophys. J. 91, 4180–4190. https://doi.org/10.1529/biophysj.106.084293.

Pelosi, P., Maida, R., 1995. Odorant-binding proteins in insects. Comp. Biochem. Physiol. 111, 503–514. https://doi.org/10.1016/S0083-6729(10)83010-9.

Pelosi, P., Zhou, J.J., Ban, L.P., Calvello, M., 2006. Soluble proteins in insect chemical communication. Cell. Mol. Life Sci. 63, 1658–1676. https://doi.org/10.1007/s00018-005-5607-0.

Pesenti, M.E., Spinelli, S., Bezirard, V., Briand, L., Pernollet, J.C., Tegoni, M., Cambillau, C., 2008. Structural basis of the honey bee PBP pheromone and pH-induced conformational change. J. Mol. Biol. 380, 158–169. https://doi.org/10.1016/j.jmb.2008.04.048.

Pickett, J.A., Allemann, R.K., Birkett, M.A., 2013. The semiochemistry of aphids. Nat. Prod. Rep. 30, 1277. https://doi.org/10.1039/c3np70036d.

Pickett, J.A., Griffiths, D.C., 1980. Composition of aphid alarm pheromones. J. Chem. Ecol. 6, 349–360. https://doi.org/10.1007/BF01402913.

Plettner, E., Lazar, L., Prestwich, E.G., Prestwich, G.D., 2000. Discrimination of pheromone enantiomers by two pheromone binding proteins from the gypsy moth Lymantria dispar. Biochemistry 39, 8953–8962.

Puchner, C., Eixelsberger, T., Nidetzky, B., Brecker, L., 2015. Saturation transfer difference NMR to study substrate and product binding to human UDP-xylose synthase (hUXS1A) during catalytic event. RSC Adv. 5, 86919–86926. https://doi.org/10.1039/c5ra18284k.

Qiao, H., Tuccori, E., He, X., Gazzano, A., Field, L., Zhou, J.J., Pelosi, P., 2009. Discrimination of alarm pheromone (E)-β-farnesene by aphid odorant-binding proteins. Insect Biochem. Mol. Biol. 39, 414–419. https://doi.org/10.1016/j.ibmb.2009.03.004.

Schreiber, S.L., Meyers, H.V., Wibery, K.B., 1986. Stereochemistry of the intramolecular enamine/enal (enone) cycloaddition reaction and subsequent transformations. J. Am. Chem. Soc. 108, 8274–8277.

Schrödinger, L., 2015. The PyMOL Molecular Graphics System.

Sun, Y.F., de Biasio, F., Qiao, H.L., Iovinella, I., Yang, S.X., Ling, Y., Riviello, L., Battaglia, D., Falabella, P., Yang, X.L., Pelosi, P., 2012. Two odorant-binding proteins mediate the behavioural response of aphids to the alarm pheromone (e)-ß-farnesene and structural analogues. PLoS One 7, 1–10. https://doi.org/10.1371/journal.pone.0032759.

Touchet, S., Chamberlain, K., Woodcock, C.M., Miller, D.J., Birkett, M.A., Pickett, J.A., Allemann, R.K., 2015. Novel olfactory ligands via terpene synthases. Chem. Commun. 51, 7550–7553. https://doi.org/10.1039/C5CC01814E.

Vogt, R.G., Riffiford, L.M., 1981. Pheromone binding and inactivation by moth antennae. Nature 293, 161–163.

Wang, Q., Liu, J.-T., Zhang, Y.-J., Chen, J.-L., Li, X.-C., Liang, P., Gao, X.-W., Zhou, J.-J., Gu, S.-H., 2021. Coordinative mediation of the response to alarm pheromones by three odorant binding proteins in the green peach aphid Myzus persicae. Insect Biochem. Mol. Biol. 130, 103528 https://doi.org/10.1016/j.ibmb.2021.103528.

Wojtasek, H., Hansson, B.S., Leal, W.S., 1998. Attracted or repelled? - a matter of two neurons, one pheromone binding protein, and a chiral centre. Biochem. BioPh. Res. Co. 250, 217–222.

Xia, Y., Zhu, Q., Jun, K.Y., Wang, J., Gao, X., 2010. Clean STD-NMR spectrum for improved detection of ligand-protein interactions at low concentration of protein. Magn. Reson. Chem. 48, 918–924. https://doi.org/10.1002/mrc.2687.

Zhang, R., Wang, B., Grossi, G., Falabella, P., Liu, Y., Yan, S., Lu, J., Xi, J., Wang, G., 2017. Molecular basis of alarm pheromone detection in aphids. Curr. Biol. 27, 55–61. https://doi.org/10.1016/j.cub.2016.10.013.

Zhou, J.J., Robertson, G., He, X., Dufour, S., Hooper, A.M., Pickett, J.A., Keep, N.H., Field, L., 2009. Characterisation of Bombyx mori odorant-binding proteins reveals that a general odorant-binding protein discriminates between sex pheromone components. J. Mol. Biol. 3 (12), 529–545.

Zhou, J.J., Vieira, F.G., He, X.L., Smadja, C., Liu, R., Rozas, J., Field, L.M., 2010. Genome annotation and comparative analyses of the odorant-binding proteins and chemosensory proteins in the pea aphid *Acyrthosiphon pisum*. Insect Mol. Biol. 19, 113–122. https://doi.org/10.1111/j.1365-2583.2009.00919.x.

Zhu, G.H., Xu, J., Cui, Z., Dong, X.T., Ye, Z.F., Niu, D.J., Huang, Y.P., Dong, S.L., 2016. Functional characterization of SlitPBP3 in Spodoptera litura by CRISPR/Cas9 mediated genome editing. Insect Biochem. Mol. Biol. 75, 1–9. https://doi.org/10.1016/j.ibmb.2016.05.006.